

# Fractional Electromagnetic Response in Three-Dimensional Chiral Anomalous Semimetal

Huan-Wen Wang, Bo Fu, Jin-Yu Zou, Zi-Ang Hu, Shun-Qing Shen\*

*Department of Physics, The University of Hong Kong, Pokfulam Road, Hong Kong, China*

(Dated: February 7, 2022)

The magnetoelectric coupling of electrons in a three-dimensional solid can be effectively described by axion electrodynamics. Here we report the discovery of the fractional magnetoelectric effect in chiral anomalous semimetals of the three-dimensional massless Wilson fermions, which have linear dispersions at the energy crossing point, and break the chiral symmetry at generic momenta. In the presence of electric and magnetic fields, the time-reversal and parity symmetry breaking give rise to the quarter-quantized topological magnetoelectric effect, which is directly related to the winding number  $1/2$  of the band structure, and is only one half of that for topological insulators. The fractional electromagnetic response can be revealed by the surface Hall conductance and extracted from the measurement of the topological Kerr and Faraday rotation. The transition-metal pentatelluride  $\text{ZrTe}_5$  with a strain-tunable band gap provides a potential platform to test the effect experimentally.

*Introduction* The electromagnetic response of a three-dimensional insulator is described by an effective axion action  $S_\theta = \frac{\theta}{2\pi} \frac{e^2}{\hbar} \int d^3x dt \mathbf{E} \cdot \mathbf{B}$  in addition to the conventional Maxwell action [1]. Here  $\mathbf{E}$  and  $\mathbf{B}$  are the electromagnetic fields inside the insulator, and  $\theta$  is the axion field. All time-reversal invariant insulators fall into two distinct classes described by either  $\theta = 0$  (for trivial insulators) or  $\theta = \pm\pi$  (for topological insulators) [2, 3]. The time reversal invariance of topological insulator makes the  $\theta$ -term quantized and leads to the topological magnetoelectric effect in units of fine structure constant  $\alpha = e^2/\hbar c$  [4–6]. In general, the axion field  $\theta$  can be evaluated from the zero-field non-Abelian Berry connection of the band structure as  $\theta = \frac{1}{4\pi^2} \int_{BZ} d^3k \epsilon^{lmn} \text{Tr}[\mathcal{A}_l \partial_m \mathcal{A}_n - \frac{2i}{3} \mathcal{A}_l \mathcal{A}_m \mathcal{A}_n]$ , where  $\mathcal{A}_l^{\mu\nu} = i \langle u_\mu | \partial_l u_\nu \rangle$  is the Berry connection defined from the Bloch function of occupied band  $\mu$  and  $\nu$ ,  $\epsilon^{lmn}$  is the Levi-Civita symbol, the indices  $l, m, n$  run over 1, 2, 3 and  $\partial_l = \partial/\partial k_l$  [2, 6]. This Chern-Simons contribution to the magnetization remains parallel to electric field for arbitrary orientations of the external field relative to the crystal axes and vanishes in less than three dimensions. With an open boundary condition, the topological magnetoelectric effect corresponds to the half-quantized surface Hall conductance subjected to a symmetry-broken Zeeman field [2, 7]. Now a question on the validity of the axion action arises when the band gap of the system closes. Furthermore, even if the action exists, what is the value of the action  $\theta$ ? Does the surface Hall effect still hold? These are the key issues that we want to address in the present work.

Massless Wilson fermions arise from the lattice regularization for Dirac fermions in the lattice gauge theory, which possess the linear dispersion near the energy crossing point, but breaks the chiral symmetry at higher energy [8–10]. The massless Wilson fermions may constitute a novel type of topological quantum semimetal, named chiral anomalous semimetal (CAS). This topological phase violates the Nielsen-Ninomiya or fermion dou-

bling theorem [9] and is characterized by a one-half topological invariant. This is opposite to all existing topological phases, such as quantum Hall effect, topological insulators and topological superconductors, which are always characterized by integer topological invariants, i.e.,  $\mathbb{Z}$  or  $\mathbb{Z}_2$  index [3, 11–17]. In this Letter, we present the derivation of the  $\theta$  field for CAS in the presence of electromagnetic field. The value of  $\theta$  is found to be  $\pm\pi/2$  subjected to the time-reversal and parity symmetry breaking, leading to a quarter-quantized topological magnetoelectric effect. The  $\theta$  field and spatial distribution of magnetoelectric polarization can be revealed by the surface Hall conductance, although there is no surface state, and extracted from the measurement of the topological Kerr and Faraday rotation at reflectivity minimum and maximum, which can provide a substantial evidence for the existence of CAS in solids. Lastly, the interaction, strain and temperature tunable axion field have been discussed near the topological phase transition point in transition-metal pentatelluride  $\text{ZrTe}_5$ .

*Model Hamiltonian* In electronic system, the CAS states can be realized near the topological phase transition points. The first principles calculation and the angle-resolved photoemission spectroscopy (ARPES) measurement demonstrate that the band structures of transition-metal pentatelluride  $\text{ZrTe}_5$  is the prototype of massive Dirac material [18–22], which is very close to the critical points. In the basis ( $|\text{Te}_1 p_y \uparrow\rangle, |\text{Te}_1 p_y \downarrow\rangle, |\text{Te}_2 p_y \uparrow\rangle, |\text{Te}_2 p_y \downarrow\rangle$ ), with  $\text{Te}_{1/2} p_y$  being the  $p_y$  orbital of the two Te atoms in the unit cell, the low energy  $\mathbf{k} \cdot \mathbf{p}$  Hamiltonian can be described by the following modified Dirac equation [18, 19, 23]

$$H_0(k) = (m - b\hbar^2 k^2)\tau_1 + v\hbar(k_1\tau_3\sigma_3 + k_2\tau_2 + k_3\tau_3\sigma_1), \quad (1)$$

where  $v$  is the effective velocity,  $k_i$  with  $i = 1, 2, 3$  are the wavevector operators.  $\sigma = \{\sigma_1, \sigma_2, \sigma_3\}$  and  $\tau = \{\tau_1, \tau_2, \tau_3\}$  are the Pauli matrices acting on the spin and orbital space, respectively.  $m - b\hbar^2 k^2$  is the momentum-dependent Dirac mass. It was found experimentally that

the band gap  $m$  varies linearly with strain near the Dirac point and can be tuned to change its sign by external strain [21, 22]. Here we focus on the case of semi-metallic state ( $m = 0$ ). When  $b = 0$  and  $m = 0$ , Eq. (1) describes the massless Dirac fermion with linear dispersion, and it has the chiral symmetry with chiral operator  $\gamma_5 = \tau_2\sigma_2$ , which is forbidden in a lattice case. When  $b \neq 0$  and  $m = 0$ , Eq. (1) describes the CAS. The presence of the  $b$  term in Eq. (1) breaks the chiral symmetry  $[\gamma_5, \tau_1] \neq 0$  explicitly. However, the system still possesses an additional sublattice symmetry as  $(\tau_3\sigma_2)H_0(\tau_3\sigma_2) = -H_0$ . Under the rotation transformation in the orbital and spin space  $\mathcal{U} = \exp(i\frac{\pi}{3}\tau \cdot \hat{n}) \exp(i\frac{\pi}{4}(\tau_0\sigma_2 + \tau_1\sigma_2))$ , where  $\hat{n}$  is the unit vector along the direction (1, 1, 1),  $H_0$  is brought into an off-diagonal form as  $\begin{pmatrix} 0 & q \\ q^\dagger & 0 \end{pmatrix}$  with  $q = v\hbar\mathbf{k} \cdot \sigma' + ib\hbar^2(\mathbf{k} \cdot \sigma')^2$  and  $\sigma' = \{\sigma_1, \sigma_2, -\sigma_3\}$ . Then, the topological property of  $H_0$  can be characterized by the three-dimensional winding number [24, 25]  $w_{3D} = \int \frac{d^3\mathbf{k}}{24\pi^2} \epsilon^{lmn} \text{tr}[(\hat{q}^{-1}\partial_l\hat{q})(\hat{q}^{-1}\partial_m\hat{q})(\hat{q}^{-1}\partial_n\hat{q})]$ , where  $\hat{q} = \frac{v\hbar\mathbf{k} \cdot \sigma + ib\hbar^2(\mathbf{k} \cdot \sigma)^2}{\sqrt{v^2\hbar^2k^2 + b^2\hbar^4k^4}}$ . After some tedious algebra, one finds

$$w_{3D} = -\frac{1}{2} \text{sgn}(b). \quad (2)$$

Hence, the CAS is strikingly distinct from the existing topological phases with integer topological invariants. In general, the half-quantized winding number can be ascribed to the chiral symmetry around the energy crossing point and is classified by the relative homotopy group.

After carefully examining numerically and analytically, we find no evidence to support the existence of the surface states around the CAS in contrast to the topological insulators. As shown in Ref. [25], the integer winding number is related to the half-quantized orbital magnetoelectric polarization in the presence of sublattice symmetry for a gapped system. Then, one natural question raises here: does the one-half winding number indicate a quarter-quantized orbital magnetoelectric polarization in the absence of the surface states?

*Fractional orbital magnetoelectric polarization* To explore the magnetoelectric effect, we begin with the Landau levels of the CAS in a finite magnetic field  $B$  along the  $z$  direction by including a symmetry breaking term  $m_2\tau_3\sigma_2$ , which destroys both the time-reversal and spatial inversion symmetry but preserves their combination [26, 27]. The term acts as the spin density wave order and will be discussed later. To find the solution of Landau levels, we make a unitary transformation  $\mathcal{U}$  for the original Hamiltonian as  $\mathcal{U}^\dagger H \mathcal{U} = -\tau_2 b (\Pi \cdot \sigma')^2 + \tau_1 v \Pi \cdot \sigma' - m_2 \tau_3$ . The momentum operators  $\hbar k_i$  are replaced by kinematic momentum operators  $\Pi_i = \hbar k_i + e A_i$  under the Pirls substitution, where  $A_i$  is  $i$ th component of the vector potential. Without loss of generality, one can choose the vector potential as  $A_i = -\delta_{i1} B y$  and  $\delta_{ij}$  the Kronecker delta symbol. By taking advantage of the

ladder operator technique [29], we can obtain the eigenvalues and eigenstates for the operator,

$$\Pi \cdot \sigma' |n, k_1, k_3, \chi_n\rangle = \chi_n \sqrt{\hbar^2 k_3^2 + n\hbar^2 \Omega^2 / v^2} |n, k_1, k_3, \chi_n\rangle \quad (3)$$

where  $n = 0, 1, 2, \dots$  are the indices of the Landau levels, and  $\Omega \equiv \sqrt{2}v\ell_B^{-1}$  is the cyclotron frequency with the magnetic length  $\ell_B = \sqrt{\hbar/eB}$ .  $\chi_n$  stands for the helicity of massive Dirac fermions:  $\chi_n = \pm 1$  for  $n > 0$  and  $\chi_0 = \text{sgn}(k_3)$  for  $n = 0$ . Then, the energy spectra are quantized into a series of Landau levels. In fact, the lowest Landau levels are primarily responsible for the emergence of exotic quantum phenomena. In this way, we can reduce the dimension to one by projecting onto the lowest Landau levels with the Landau degeneracy  $eB/\hbar$ . The Hamiltonian and all the physical quantities can be expressed in terms of  $2 \times 2$  matrices and the motions of electrons are confined along the direction of magnetic field, *i.e.*,

$$H^{(0)} = v\hbar k_3 \tau_1 - b\hbar^2 k_3^2 \tau_2 - m_2 \tau_3. \quad (4)$$

The eigen states of the one-dimensional Hamiltonian are given by  $[se^{-i\varphi} \cos \frac{\phi_s}{2}, \sin \frac{\phi_s}{2}]^T$  for  $m_2 < 0$  and  $[s \cos \frac{\phi_s}{2}, e^{i\varphi} \sin \frac{\phi_s}{2}]^T$  for  $m_2 > 0$ , where  $e^{i\varphi} \equiv \frac{\text{sgn}(k_3)[v - ib\hbar k_3]}{\sqrt{v^2 + b^2\hbar^2 k_3^2}}$ ,  $\cos \phi_s = -\frac{sm_2}{\sqrt{v^2\hbar^2 k_3^2 + b^2\hbar^4 k_3^4 + m_2^2}}$ ,  $s = +$  for conduction band and  $s = -$  for valence band. For a given  $m_2$ , the eigen state is always well-defined in the momentum space, and the corresponding electric polarization  $-e\langle i\partial_3 \rangle$  can be calculated as  $P_z^{(0)} = -e \text{sgn}(m_2) \int_{-\infty}^{+\infty} \partial_{k_3} \varphi_0 \cos^2 \frac{\phi_{\text{sgn}(m_2)}}{2} \frac{dk_3}{2\pi}$ , which is quarter quantized as  $P_z^{(0)} = \frac{e}{4} \text{sgn}(m_2 b)$  as  $m_2 \rightarrow 0$ . Consider the Landau degeneracy  $n_B = |eB|/2\pi\hbar$ , the variation of the free energy density from the lowest Landau levels can be found as  $\Delta\mathcal{F} = eP_z^{(0)} \mathbf{E} \cdot \mathbf{B}/\hbar$ . For higher Landau levels, the contribution can be proved to vanish in the limit of  $m_2 \rightarrow 0$ . Consequently, the total  $\Delta\mathcal{F}$  becomes  $\Delta\mathcal{F} = e^2 \text{sgn}(m_2 b) \mathbf{E} \cdot \mathbf{B}/4\hbar$  as  $m_2 \rightarrow 0$ , which corresponds to a fractional  $\theta$ -term in units of  $2\pi$  as

$$\lim_{m_2 \rightarrow 0} \frac{\theta}{2\pi} = \frac{1}{2} w_{3D} \text{sgn}(m_2). \quad (5)$$

Hence,  $\frac{\theta}{2\pi}$  is quarter quantized in a finite electromagnetic field and is one half of the winding number with an additional factor  $\text{sgn}(m_2)$ . In the absence of  $m_2$ , the model has the parity symmetry  $\tau_1 H^{(0)}(-k_3)\tau_1 = H^{(0)}(k_3)$ . Due to the double degeneracy of the zeroth Landau bands, the two orthogonal states at the  $k_3 = 0$  can be expressed as superpositions of the odd-parity and even-parity states. The coefficient  $\text{sgn}(m_2)$  indicates that the spontaneous symmetry breaking of the electric polarization induced by the external perturbation  $m_2\tau_2$ . The sign of  $m_2$  determines the occupancy of the degenerated states. Thus the  $\theta$  field emerges in the gapless CAS as a consequence of spontaneous symmetry breaking induced by an infinitesimal small field  $m_2$ .

*Surface Hall conductance* The nonzero value of the field  $\theta$  in the bulk means the emergence of the surface Hall effect on the surface of the system. To explore the surface Hall effect of CAS, the continuum Hamiltonian (1) is discretized on a cubic lattice by the replacement  $k_i \rightarrow \sin k_i$  and  $k_i^2 \rightarrow 4 \sin^2 \frac{k_i}{2}$  in a unit lattice spacing. Consider a slab geometry that is finite in the  $z$ -direction, and perform the periodic condition along the  $x$  and  $y$  directions. The surface Hall effect can be resolved by the layer-dependent Hall conductance as [6, 30]

$$\sigma_{xy}(\ell) = \frac{e^2}{h} \frac{1}{2\pi} \sum_{\ell'} \int dk_x dk_y \sum_{m,n} \frac{2\text{Im}[v_{nm}^x(\ell)v_{mn}^y(\ell')]}{(E_n - E_m)^2}, \quad (6)$$

where  $\ell$  labels the layer index along the  $z$  direction,  $n$  and  $m$  label the occupied and unoccupied bands, respectively.  $v_{nm}^i(\ell) \equiv \langle \varphi_n(k_x, k_y) | \partial_i H_\ell | \varphi_m(k_x, k_y) \rangle$  are the matrix elements of local velocity operators along the  $i$ -direction with  $i = x, y$ ,  $H_\ell = \sum_{s,s'} \langle \ell, s | (H_0 + m_2 \tau_2) | \ell, s' \rangle | \ell, s \rangle \langle \ell, s' |$  projects out the  $\ell$ th sector of the Hamiltonian,  $s$  and  $s'$  denote the spin or orbital indices. According to the topological field theory [2], the value of  $\theta$  in the vacuum is  $\theta = 0$ . The axion field will decay near the sample surface, and the bulk properties of  $\theta$  in unit of  $2\pi$  can be deduced from the surface Hall conductance  $\sigma_{xy}$

$$\frac{\theta_f}{2\pi} = -\frac{\hbar}{e^2} \sum_{\ell'=1}^{N_L/2} \sigma_{xy}(\ell'). \quad (7)$$

Here we have used the symbol  $\theta_f$  to distinguish with the  $\theta$  calculated from the periodic boundary condition, and the subscript  $f$  means finite size.  $N_L$  is the total number of layers along the  $z$ -direction. For a slab with finite thickness,  $\theta_f$  is a function of  $N_L$ . In the thermodynamic limit  $N_L \rightarrow +\infty$ ,  $\theta_f$  becomes  $\theta$  [30]. It is noted that  $\frac{\theta}{2\pi}$  evaluated from the non-Abelian Berry curvature is ambiguous up to an integer, while  $\frac{\theta_f}{2\pi}$  from Eq. (7) is always unambiguous. Hence, it is more proper to define the  $\theta$ -term from the layer-dependent Hall conductance in real materials.

To reveal the relation between  $\theta$  and  $\theta_f$ , we calculate the layer-dependent Hall conductance for CAS phase with finite  $m_2$ . As shown in Fig. 1(a), we have evaluated the layer-dependent Hall conductance  $\sigma_{xy}(\ell)$  as a function of layer index  $\ell$  for several different total layer numbers  $N_L = 8, 16, 24, 36, 48$ , and the layer index is labeled from  $-N_L/2 + 1$  to  $N_L/2$ . It is noted that the  $\sigma_{xy}(\ell)$  is localized around the surface. Its magnitude has a maximum at the top and bottom layers and gradually decreases to 0 in the bulk, and the corresponding penetration depth is around 10 layers for the selected model parameters. As depicted in Fig. 1(b), the dimensionless parameters  $\theta_f$  deduced from Fig. 1(a) tends to be saturated to a constant  $\theta$  by fixing  $m_2 = 0.2$  when the total layer number  $N_L \rightarrow +\infty$ . For a given total layer number, for example,  $N_L = 16$ , the penetration depth of layer

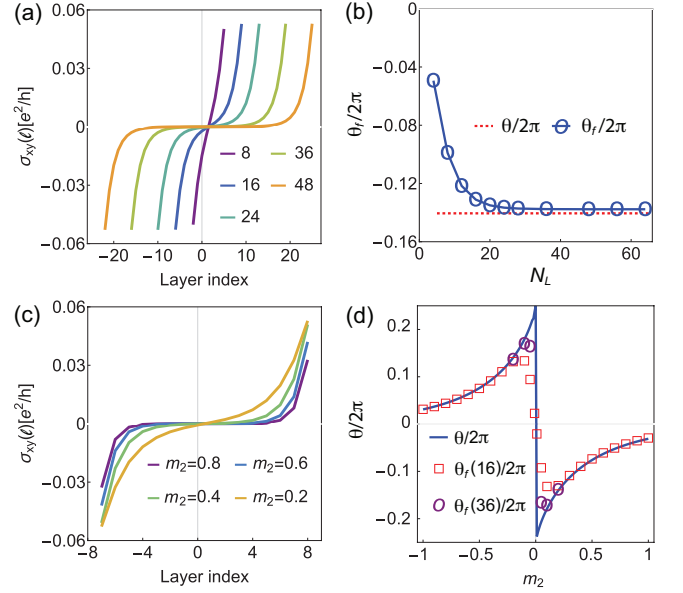


Figure 1. (a) Layer-dependent Hall conductance in units of  $e^2/h$  as a function of layer index for CAS with different total layer numbers ( $N_L = 8, 16, 24, 36, 48$ ). (b) The extracted  $\theta_f$  (blue circles) as function of  $N_L$  and  $\theta$  (red dashed line). (c) Layer-dependent Hall conductance for CAS with different  $m_2$  (0.2, 0.4, 0.6, 0.8). (d) Comparison of  $\theta$  and extracted  $\theta_f$  as functions of  $m_2$ . In (a) and (b),  $m_2$  is fixed as  $m_2 = 0.2$ . In (c),  $N_L$  is fixed as  $N_L = 16$ . Other calculation parameters are chosen as  $b = 0.5$  in (a-d).

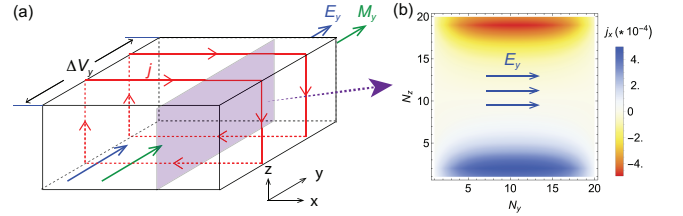


Figure 2. (a) Schematic diagram of the relation between magnetization and bulk topological magnetoelectric effect. A surface current is produced by an electric field due to the magnetization. (b) Local current density along the  $x$ -direction in the  $y-z$  plane. The electric field is applied along the  $y$ -direction. The calculation parameters are chosen as  $m = 0$ ,  $m_2 = 0.2$ ,  $b = 0.5$ .

Hall conductance decreases with increasing  $m_2$  as shown in Fig. 1(c). Meanwhile, the extract  $\theta_f$  from the  $\sigma_{xy}(\ell)$  is more closed to  $\theta$  with increasing  $m_2$  as shown in Fig. 1(d). For small  $m_2$ , a larger layer number is required to make  $\theta_f$  approaching  $\theta$ .

Opposite the conventional topological insulator, there is no corresponding well-defined surface states for CAS with finite  $m_2$ , although there is a layer-dependent Hall conductance. The  $m_2$  term breaks the time reversal symmetry and causes a bulk band gap. The generation of electric current near the sample surface can be regarded

as a consequence of the magnetoelectric effect. For illustration, we consider a cuboid geometry in Fig. 2(a), and there is a voltage difference  $\Delta V_y$  along the  $y$ -direction, which corresponds to a constant electric field  $E_y$  (blue arrow). The axion action  $S_\theta = \frac{e^2}{h} \int d^3x dt \frac{\theta}{2\pi} \mathbf{E} \cdot \mathbf{B}$  tells us that the electric field will produce a magnetization as  $\mathbf{M} = \theta e^2/(4\pi^2\hbar) \mathbf{E}$  (green arrow); then, the magnetization will produce a current near the surface as  $\mathbf{j} = \nabla \times \mathbf{M} = e^2/(4\pi^2\hbar) \nabla\theta \times \mathbf{E}$  (red arrow), which is perpendicular to the direction of electric field [2]. If  $\theta$  is uniform inside the material and is 0 for the vacuum,  $\nabla\theta \neq 0$  only at the boundary; hence, the current exactly flows at the surface of cuboid as indicated by the red arrow in Fig. 2(a). For finite-size cuboid,  $\theta$  will be a function of the position even inside the cuboid, and there is a penetration length for the magnetization current. The above argument can be numerically verified by evaluating the local current density along the  $x$ -direction in the  $y-z$  plane, as indicated by the purple plane in Fig. 2(a). For simplicity, we assume there is a periodic boundary condition in the  $x$  direction. By attaching the electrodes on the  $y$  direction, the Hamiltonian is modified to  $H(k_x, y, z) \rightarrow H_0(k_x, y, z) + m_2\tau_2 + \Delta V \mathbb{I}_{4 \times 4}$ , where  $\Delta V = -eE_y y$  gives the potential difference between the two electrodes on the  $y$  direction [31],  $\mathbb{I}_{4 \times 4}$  is the  $4 \times 4$  identity matrix. The current density  $j_x(y, z)$  is given by the expectation value of the local current operator  $\hat{j}_x(y, z) = \frac{e}{\hbar} \sum_{ss'} \langle yzs | \partial_{k_x} H | yzs' \rangle | yzs \rangle \langle yzs' |$  as  $j_x(y, z) = \int \frac{dk_x}{2\pi} \sum_n \langle \varphi_n(k_x) | \hat{j}_x(y, z) | \varphi_n(k_x) \rangle$ , where  $|\varphi_n(k_x)\rangle$  is the occupied Bloch states. As shown in Fig. 2(b), the local current density mainly distributes near the top and bottom few layers, and nearly vanishes inside the deep bulk. Consistent with the layer-dependent Hall conductance, the local current density has opposite sign on the top and bottom surfaces, the total current density is zero for the whole bar sample.

For comparison, we also present the results for topological insulators by considering  $m \neq 0$  in Eq. 1. It is known that  $mb > 0$  describes the topological insulators and  $mb < 0$  describes the trivial insulators [32]. For nonzero  $m_2$ ,  $\frac{\theta}{2\pi}$  is a function of  $m$  and  $m_2$  for a given  $b$  as shown in Fig. 3(a), and it always satisfies the relation as  $\frac{\theta}{2\pi} \propto \text{sgn}(m_2)$ . When  $m_2 \rightarrow 0$ ,  $\frac{\theta}{2\pi}$  can be analytically found as  $\frac{\theta}{2\pi} = -\frac{1}{4}[\text{sgn}(m) + \text{sgn}(b)]\text{sgn}(m_2)$ . Hence,  $\frac{\theta}{2\pi}$  is half-quantized as  $\pm 1/2$  or 0 for a finite  $m$  and  $b$  in the absence of  $m_2$ , while  $\frac{\theta}{2\pi}$  is quarter-quantized as  $\pm 1/4$  for  $m = 0$  and  $m_2 \rightarrow 0$ . Similar to Fig. 1(c), we give the relation between  $\theta$  and  $\theta_f$  as a function of  $m_2$  in Fig. 3(b) for topological insulators ( $m = 1$ ). In such a case, the  $\sigma_{xy}(\ell)$  is well-localized around the sample surface, and there is a good agreement between  $\theta$  and  $\theta_f$  when  $N_L = 16$ .

*Topological Kerr and Faraday rotation* Physically, the action  $S_\theta$  modifies the Maxwell's equations and leads to unusual optical properties, such as the topological

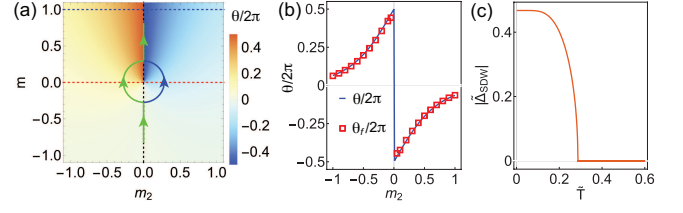


Figure 3. (a) Phase diagram of  $\theta$  as functions of  $m_2$  and  $m$ . Other parameters are chosen as  $v = 1$  and  $b = 0.5$ . (b) Comparison of  $\theta$  and extracted  $\theta_f$  as functions of  $m_2$  for topological insulator for  $m = 1$ . (c) The amplitude of  $\tilde{\Delta}_{SDW}$  as a function of dimensionless temperature  $\tilde{T}$ , which is solved numerically from Eq. (S3). The dimensionless mass and coupling constant are chosen as  $\tilde{m} = -0.2$  and  $\tilde{g}_{SDW} = 1.3$ , respectively.

Kerr and Faraday rotations, which provide an effective way to measure the magnetoelectric polarization in solids [33–35]. Near the boundary between CAS ( $\theta_{CAS}$ ) and vacuum ( $\theta = 0$ ), the surface Hall conductance becomes  $\sigma_{xy}^{T(B)} = \frac{e^2}{h} \nu_{T(B)}$ , where  $\nu_T = -\frac{\theta_{CAS}}{2\pi}$  and  $\nu_B = \frac{\theta_{CAS}}{2\pi}$ . The two surface Hall conductance can be related to the magneto-optical measurement. One can extract the information of  $\theta_{CAS}$  through an optical measurement. In experiments, there is a normally incident linearly  $x$ -polarized light propagating along the  $z$  direction. The Kerr and Faraday angle at reflectivity minimum and maximum are obtained as  $\theta'_{K,F}$  and  $\theta''_{K,F}$ , respectively. As  $\nu_B + \nu_T = 0$ , we have  $2\alpha P_3^{CAS} = \tan(\theta''_K + \theta'_F)$  [35]. We expect the obtained  $\theta_{CAS}$  approaches the quantized value  $\pm\pi/2$  as  $m_2 \rightarrow 0$ , which can provide a substantial evidence for the existence of CAS in solids.

*Physical realization of  $m_2$*  The symmetry breaking term  $m_2\tau_3\sigma_2$  can be realized by a staggered Zeeman field pointing in the  $y$  direction on the sublattice  $\text{Te}_1$  and  $\text{Te}_2$  of each unit cell. This Zeeman field can be produced by a spin density wave order, where spins point along opposite  $y$  directions on two sublattices. In the mean field approximation, the system can develop spin density wave order  $\Delta_{SDW}$  if the effect of on-site repulsion  $H_U = U \sum_i (n_{iA\uparrow} n_{iA\downarrow} + n_{iB\uparrow} n_{iB\downarrow})$  dominates that of inter-site repulsion  $H_V = V \sum_{i,\sigma} n_{iA\sigma} n_{iB\sigma}$  with  $A/B = \text{Te}_{1/2} p_y$  [23, 26, 27]. As the spin density wave order enters the Hamiltonian (1) as  $\delta H = \Delta_{SDW} \tau_3 \sigma_2$ , it indeed produces the desired symmetry breaking term [28]. Moreover, we will show that such a spin density wave order can be tuned by external strain. By introducing the dimensionless parameters  $\tilde{g}_{SDW} = \frac{U\Lambda^2}{16\pi^2(\hbar v)^3}$ ,  $\tilde{\Delta}_{SDW} = \frac{\Delta_{SDW}}{\Lambda}$ ,  $\tilde{m} = m/\Lambda$  with  $\Lambda$  the energy cutoff, the critical value for the coupling strength is determined as  $\tilde{g}_{SDW}^c(\tilde{m}) = (\sqrt{\tilde{m}^2 + 1} - \tilde{m}^2 \tanh^{-1} \frac{1}{\sqrt{\tilde{m}^2 + 1}})^{-1}$ , which is a monotonic increasing function of  $|\tilde{m}|$  [23]. Depending on the coupling strength  $\tilde{g}_{SDW}$ , there exists two distinct regimes as we change the strain (which modi-

fies the Dirac mass effectively). When  $\tilde{g}_{SDW} < 1$ , as  $\tilde{g}_{SDW}^c(\tilde{m}) \geq \tilde{g}_{SDW}^c(0) = 1$ ,  $\tilde{g}_{SDW}^c(\tilde{m}) > \tilde{g}_{SDW}$  is satisfied regardless of the mass  $\tilde{m}$ ,  $\tilde{\Delta}_{SDW}$  is always zero by varying the strain. When  $\tilde{g}_{SDW} > 1$ , there exists the spin density wave instability once  $\tilde{g}_{SDW} > \tilde{g}_{SDW}^c$ . Considering the order parameter and Dirac mass are small compared with  $\Lambda$ , the  $\tilde{\Delta}_{SDW}$  at zero temperature can be solved approximately as [23]

$$\tilde{\Delta}_{SDW}^2 + \tilde{m}^2 \approx (\tilde{g}_{SDW} - 1)^{1.266}. \quad (8)$$

Without loss of generality, we can assume the material is a weak topological insulator and  $\tilde{g}_{SDW}^c(\tilde{m}) > \tilde{g}_{SDW}$  in the absence of strain. By increasing the strain, the  $|\tilde{m}|$  and  $\tilde{g}_{SDW}^c(\tilde{m})$  decrease simultaneously when  $\tilde{m} < 0$ . When  $|\tilde{m}|$  is smaller than the critical value  $|\tilde{m}_c|$  with  $\tilde{g}_{SDW}^c(\tilde{m}_c) = \tilde{g}_{SDW}$ , the order parameter  $\tilde{\Delta}_{SDW}$  becomes nonzero and breaks the time-reversal and inversion symmetry spontaneously. With further increasing of the strain,  $\tilde{\Delta}_{SDW}$  grows following the relation (8). Then, the corresponding axion field will be tuned along the green or blue line in Fig. 3(a), which is a semicircle as  $|\tilde{m}| < |\tilde{m}_c|$ . For vanishing Dirac mass  $\tilde{m} = 0$ ,  $\tilde{\Delta}_{SDW}$  reaches its maximum. When the strain is large enough that the  $\tilde{m} \geq |\tilde{m}_c|$ ,  $\tilde{\Delta}_{SDW}$  vanishes again and the system becomes a strong topological insulator. It is noted that the bulk energy gap closing is avoided due to the finite spin density wave order in the process of topological phase transition. Besides, as shown in Fig. 3(c), the order parameter decreases with increasing the temperature below the critical temperature, which might provide another way to tune the axion field in Fig. 3(a) by reducing the radius of green and blue line. Hence, the CAS states near  $\tilde{m} = 0$  has a natural advantage in generating axion field by introducing interaction, strain and temperature.

This work was supported by the National Key R&D Program of China under Grant No. 2019YFA0308603 and the Research Grants Council, University Grants Committee, Hong Kong under Grant No. 17301220.

H.W.W and B.F. contributed equally to this work.

---

\* sshen@hku.hk

- [1] F. Wilczek, Two applications of axion electrodynamics, Phys. Rev. Lett. **58**, 1799 (1987).
- [2] X. L. Qi, T. L. Hughes, and S. C. Zhang, Topological field theory of time-reversal invariant insulators, Phys. Rev. B **78**, 195424 (2008).
- [3] X. L. Qi, and S. C. Zhang, Topological insulators and superconductors, Rev. Mod. Phys. **83**, 1057 (2011).
- [4] N. A. Spaldin and M. Fiebig, The renaissance of magnetoelectric multiferroics, Science **309**, 391 (2005).
- [5] M. Fiebig, Revival of the magnetoelectric effect, J. Phys. D **38**, R123 (2005).
- [6] A. M. Essin, J. E. Moore, and D. Vanderbilt, Magneto-electric polarizability and axion electrodynamics in crystalline insulators, Phys. Rev. Lett. **102**, 146805 (2009).
- [7] R. L. Chu, J. Shi, and S. Q. Shen, Surface edge state and half-quantized Hall conductance in topological insulators, Phys. Rev. B **84**, 085312 (2011).
- [8] K. G. Wilson, in New Phenomena in Subnuclear Physics, edited by A. Zichichi, (Plenum, New York, 1977).
- [9] H. B. Nielsen, and M. Ninomiya, No go theorem for regularizing chiral fermions, Phys. Lett. **B105** 219 (1981).
- [10] H. J. Rothe, Lattice Gauge Theories (World Scientific, Singapore, 1998).
- [11] Klitzing, K. v., Dorda, G. & Pepper, M. New Method for High-Accuracy Determination of the Fine-Structure Constant Based on Quantized Hall Resistance, Phys. Rev. Lett. **45**, 494 (1980).
- [12] K. v. Klitzing et al. 40 years of the quantum Hall effect, Nat. Rev. Phys. **2**, 397 (2020).
- [13] J. E. Moore, The birth of topological insulators, Nature **464**, 194 (2010)
- [14] M. Z. Hasan, and C. L. Kane, Colloquium: topological insulators, Rev. Mod. Phys. **82**, 3045 (2010)
- [15] N. P. Armitage, E. J. Mele, and A. Vishwanath, Weyl and Dirac semimetals in three-dimensional solids, Rev. Mod. Phys. **90**, 015001 (2018).
- [16] S. Q. Shen, *Topological Insulators: Dirac Equation in Condensed Matter*, 2nd ed. (Springer, Singapore, 2017).
- [17] Y. Tokura, K. Yasuda & A. Tsukazaki, Magnetic topological insulators, Nat. Rev. Phys. **1**, 126 (2019).
- [18] H. Weng, X. Dai, and Z. Fang, Transition-metal pentatelluride ZrTe<sub>5</sub> and HfTe<sub>5</sub>: A paradigm for large-gap quantum spin Hall insulators, Phys. Rev. X **4**, 011002 (2014).
- [19] R. Y. Chen, Z. G. Chen, X.-Y. Song, J. A. Schneeloch, G. D. Gu, F. Wang, and N. L. Wang, Magnetoinfrared Spectroscopy of Landau Levels and Zeeman Splitting of Three-Dimensional Massless Dirac Fermions in ZrTe<sub>5</sub>, Phys. Rev. Lett. **115**, 176404 (2015).
- [20] Q. Li, D. E. Kharzeev, C. Zhang, Y. Huang, I. Pletikosic, A. V. Fedorov, R. D. Zhong, J. A. Schneeloch, G. D. Gu, and T. Valla, Chiral magnetic effect in ZrTe<sub>5</sub>, Nat. Phys. **12**, 550 (2016).
- [21] J. Mutch, W.-C. Chen, P. Went, T. Qian, I. Z. Wilson, A. Andreev, C. C. Chen, and J. H. Chu, Evidence for a strain-tuned topological phase transition in ZrTe<sub>5</sub>, Sci. Adv. **5**, eaav9771 (2019).
- [22] P. Zhang, R. Noguchi, K. Kuroda, C. Lin, K. Kawaguchi, K. Yaji, A. Harasawa, M. Lippmaa, S. Nie, H. Weng, V. Kandyba, A. Giampietri, A. Barinov, Q. Li, G. D. Gu, S. Shin, and T. Kondo, Observation and control of the weak topological insulator state in ZrTe<sub>5</sub>, Nat. Commun. **12**, 406 (2021).
- [23] See Supplemental Material at [URL to be added by publisher] for details of S1. The  $k \cdot p$  model hamiltonian for ZrTe<sub>5</sub>, S2. The strain tunable bandgap, and S3. The spin density wave order.
- [24] A. P. Schnyder, S. Ryu, A. Furusaki, and A. W. W. Ludwig, Classification of topological insulators and superconductors in three spatial dimensions, Phys. Rev. B **78**, 195125 (2008).
- [25] S. Ryu, A. P. Schnyder, A. Furusaki, and A. W. W. Ludwig, Topological insulators and superconductors: tenfold way and dimensional hierarchy, New J. Phys. **12**, 065010 (2010).
- [26] R. Li, J. Wang, X. L. Qi, and S. C. Zhang, Dynamical axion field in topological magnetic insulators. Nat. Phys. **6**, 284(2010).

- [27] A. Sekine and K. Nomura, Axionic antiferromagnetic insulator phase in a correlated and spin-orbit coupled System. *J. Phys. Soc. Jpn.* **83**, 104709 (2014).
- [28] S. Aoki, Solution to the U(1) Problem on a Lattice, *Phys. Rev. Lett.* **57**, 3136 (1986).
- [29] S. Q. Shen, Y. J. Bao, M. Ma, X. C. Xie, and F. C. Zhang, Resonant spin Hall conductance in quantum Hall systems lacking bulk and structural inversion symmetry, *Phys. Rev. B* **71**, 155316 (2005)
- [30] J. Wang, B. Lian, X. L. Qi, and S. C. Zhang, Quantized topological magnetoelectric effect of the zero-plateau quantum anomalous Hall state, *Phys. Rev. B* **92**, 081107(R) (2015).
- [31] D. Tong, The Quantum Hall Effect, arXiv:1606.06687.
- [32] H. Z. Lu, W. Y. Shan, W. Yao, Q. Niu, and S. Q. Shen, Massive Dirac fermions and spin physics in an ultrathin film of topological insulator, *Phys. Rev. B* **81**, 115407 (2010)
- [33] J. Maciejko, X.-L. Qi, H. D. Drew, and S.-C. Zhang, Topological Quantization in Units of the Fine Structure Constant, *Phys. Rev. Lett.* **105**, 166803 (2010).
- [34] W.-K. Tse and A. H. MacDonald, Magneto-optical Faraday and Kerr effects in topological insulator films and in other layered quantized Hall systems. *Phys. Rev. B* **84**, 205327(2011).
- [35] B. Fu, Z. A. Hu, S.Q. Shen, Bulk-hinge correspondence and three-dimensional quantum anomalous Hall effect in second-order topological insulators. *Phys. Rev. Research* **3**, 033177(2021).